A flexible repertoire of transcription factor binding sites and diversity threshold determines enhancer activity in embryonic stem cells

Gurdeep Singh[1], Shanelle Mullany[1], Sakthi D Moorthy[1], Richard Zhang[1], Tahmid Mehdi[2], Virlana M Shchuka[1], Ruxiao Tian[1], Alan M Moses[1,2,3], Jennifer A Mitchell[1]*

1) Department of Cell and Systems Biology, University of Toronto, Toronto, ON, M5S 3G5, Canada.

2) Department of Computer Science, University of Toronto, Toronto, M5S 2E4, Canada.

3) Department of Ecology & Evolutionary Biology, University of Toronto, Toronto, M5S 3B3, Canada.

Key words: Enhancer; Transcription factor; Pluripotent Stem Cells; Gene expression regulation; transcription factor binding site

*** Corresponding author.**

Summary

Transcriptional enhancers are critical for development, phenotype evolution and often mutated in disease contexts; however, even in well-studied cell types, the sequence code conferring enhancer activity remains unknown. We found genomic regions with conserved binding of multiple transcription factors (TFs) in mouse and human embryonic stem cells (ESCs) are enriched in a diverse repertoire of transcription factor binding sites (TFBS) including known and novel ESC regulators. Remarkably, using a diverse set of TFBS from this repertoire was sufficient to construct short synthetic enhancers with activity comparable to native enhancers. Site directed mutagenesis of conserved TFBS in endogenous enhancers or TFBS deletion from synthetic sequences revealed a requirement for >10 different TFBS for robust activity. Specific TFBS, including the OCT4:SOX2 co-motif, are dispensable, despite co-binding the OCT4, SOX2 and NANOG master regulators of pluripotency. These findings reveal a TFBS diversity threshold overrides the need for optimized regulatory grammar and individual TFBS that bind specific master regulators.

Highlights:

- Comparative epigenomics determines the enhancer sequence code and synthetic enhancer design.
- A diversity of >10 TFBS are required and sufficient for robust enhancer activity
- >40 TFBS contribute to enhancer activity implicating new TFs in pluripotency maintenance
- Increased TFBS diversity, above a threshold, overrides the need for regulatory grammar

INTRODUCTION

Enhancers are required to regulate tissue specific gene expression during normal development. These non-coding regulatory sequences modulate inter and intra-species phenotypic divergence due to sequence variation leading to changes in gene expression (Kvon et al., 2016; McLean et al., 2011; Prescott et al., 2015). Genome-wide association

studies (GWAS) reveal that disease-associated SNPs (single nucleotide polymorphisms) are more often found in noncoding regions of the genome displaying chromatin features associated with transcriptional enhancers (Bernstein et al., 2012; Maurano et al., 2012; Visel et al., 2009a); however, the exact sequence code conferring enhancer activity remains unknown.

Extreme sequence conservation between mouse and human non-coding regions identifies active enhancers during development (Visel et al., 2008) but most mammalian enhancers do not display high sequence conservation. Enhancers active in specific cell types can be identified using chromatin features; for example, histone modifications, transcription factor (TF) or co-activator binding (Chen et al., 2012, 2008; Ernst and Kellis, 2012; Libbrecht et al., 2019; Visel et al., 2009b). Histone H3 K27 acetylation (H3K27ac) and H3 K4 monomethylation (H3K4me1) are enriched at enhancer regions, with increased H3K27ac signal associated with more active enhancers (Creyghton et al., 2010; Moorthy et al., 2017; Rada-Iglesias et al., 2011). However, predictions based on these chromatin features alone include many false positives (Barakat et al., 2018; Corces et al., 2018; Farnham, 2012; Kwasnieski et al., 2014; Visel et al., 2008, 2013) and analysis of the identified enhancers has yet to reveal a DNA sequence code that determines enhancer function. Comparative chromatin analysis of liver from 20 mammals revealed that regions with conserved H3K27ac in multiple species (Villar et al., 2015) can be exploited to identify conserved enhancer sequence properties (Chen et al., 2018).

Regions bound by multiple TFs, display increased regulatory activity by enhancer deletion, transgenic reporter assays and massively parallel reporter assays (MPRAs), compared to regions bound by single TFs (Moorthy et al., 2017; Vanhille et al., 2015; Zinzen et al., 2009). In addition, regulatory activity is higher for synthetic heterotypic sequences constructed from four different TFBS compared to homotypic sequences containing repeated TFBS (Fiore and Cohen, 2016; Smith et al., 2013). Combinatorial regulation by TFs is important for enhancer function; however, only 37% of genomic regions containing TFBS for 6 different regulatory TFs display activity (Lloret-Fernández et al., 2018). Studies of specific native enhancers and MPRAs reveal orientation and

spacing of TFBS pairs affects enhancer activity (Farley et al., 2016; Fiore and Cohen, 2016; Thanos and Maniatis, 1995). This regulatory grammar, in combination with TFBS clustering, however, does not predict which regions exhibit enhancer activity in the genome indicating we have an incomplete understanding of the regulatory code (King et al., 2020; Lusk and Eisen, 2010; Smith et al., 2013).

As regions bound by the same TF in multiple species are more likely to have regulatory activity (Ballester et al., 2014) we investigated regions with conserved binding of multiple TFs in mouse and human embryonic stem cells (ESCs) to decipher the pluripotency regulatory code. This analysis revealed a large repertoire of TFBS contribute to enhancer activity in pluripotent cells. Within individual enhancers more than 10 different TFBS are required for robust enhancer activity, indicating TFBS sequence diversity is a required feature of mammalian enhancers.

RESULTS

Comparative epigenomics reveals conserved enhancers in pluripotent stem cells contain a conserved regulatory code

To decipher the regulatory code in pluripotent cells, we investigated regions bound by multiple TFs in mouse and human ESCs (* in Figure 1A), as these regions are more likely to show enhancer activity (Ballester et al., 2014). To identify these regions, 1 kb regions bound by at least one TF in mouse were clustered based on active enhancer features: H3K27ac (Creyghton et al., 2010; Rada-Iglesias et al., 2011) and TF binding in mouse and human ESCs (Figure 1B, Table S1). The resulting clusters included regions with conserved high enhancer features (CHEF), conserved medium enhancer features (CMEF), mouse-specific high enhancer features (msHEF), and several conserved low enhancer feature (CLEF) clusters, most of which were bound by only one TF and displayed low H3K27ac in both species. The CHEF and msHEF clusters (containing the greatest enrichment for active enhancers) (Moorthy et al., 2017; Murtha et al., 2014; Schnetz et al., 2010; Zhou et al., 2014) make up only 17% of the total mouse TF bound regions and display the highest enrichment of the EP300 co-activator (Figure 1C), in

accordance with a recent MPRA revealing only 26% of TF bound regions possess enhancer activity (Barakat et al., 2018). By starting with TF bound regions in mouse we could not identify human-specific high enhancer feature (hsHEF) regions; however, clustering TF bound regions in human ESCs identified hsHEF regions, and 86.5% of the same CHEF regions identified in mouse (Figure S1A).

We next identified features that distinguished CHEF sequences from other genomic regions. CHEF sequences had increased DNA sequence conservation compared to other clusters, but could not be identified based on conservation alone (Figure 1D). As MPRA revealed that TFBS conservation, rather than overall conservation is a determinant of enhancer activity (Kheradpour et al., 2013), we analyzed matches to known transcription factor binding motifs. CHEF mouse-human TFBS conservation by comparison to scrambled TFBS indicated several TFBS are significantly conserved ($P<2.2x10^{-16}$, Wilcoxon rank-sum test, Figure S1B/C). We tested this further by evaluating TFBS conservation across six species using MotEvo (Arnold et al., 2012). As TFBS diversity is important for activity of synthetic regulatory sequences (Fiore and Cohen, 2016; Smith et al., 2013), we evaluated the number of different conserved TFBS, corresponding to ESC expressed TFs based on RNA-seq (Moorthy et al., 2017) in each of the sequences. From this set of 349 TFBS, we found CHEF sequences contain on average 12.6 conserved and different TFBS, an increased number compared to all other groups (Figure 1E). Even after removal of TFBS associated with TFs for which binding data was used to identify CHEFs, these regions contain an increased number of conserved and different TFBS compared to all other groups, suggesting there are additional regulatory TFs important in pluripotent cells (Figure S1D).

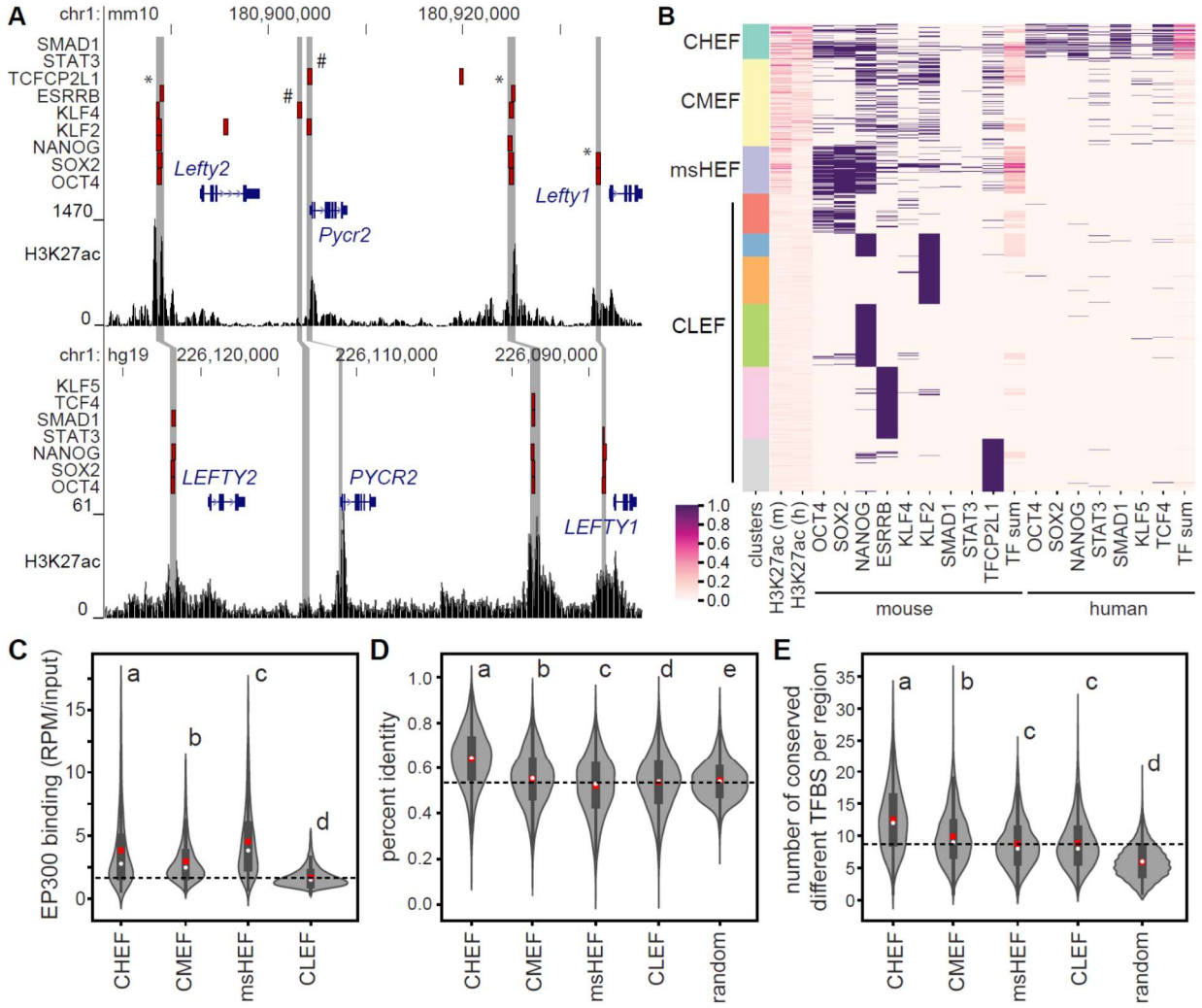

Figure 1: Conserved high enhancer feature (CHEF) regions contain a conserved regulatory code. A) The *Lefty1*/*Lefty2* locus in the mouse (top) and human (bottom) genomes. Transcription factor (TF) bound regions from ChIP-seq (red bars), mouse and human syntenic regions (grey bars), and H3K27ac ChIP-seq data are displayed on the mm10 and hg19 assemblies of the University of California at Santa Cruz (UCSC) Genome Browser. * indicates regions with conserved binding of multiple TFs in mouse and human, # indicates regions with binding only in mouse ESCs. B) Clustering of TF bound regions in mouse ESCs, using H3K27ac and TF binding at associated mouse and human regions. In C-E groups determined by one-way ANOVA to be significantly different (P<0.05) are labelled with different letters, dashed line indicates the average for the CLEF cluster. C) CHEF, CMEF and msHEF regions display significantly increased EP300 binding compared to CLEF regions. D) CHEF regions display the highest percent identity between mouse and human compared to other clusters and random non-TF bound regions. E) CHEF regions contain an increased number of conserved different TFBS compared to other clusters and random non-TF bound regions.

Conserved enhancers contain a large repertoire of TFBS required for enhancer activity

To determine the importance of specific TFBS, LASSO (least absolute shrinkage and selection operator)(Tibshirani, 1996) logistic regression was used to identify the TFBS more often present and conserved in CHEF sequences compared to the NANOG bound CLEF cluster (chosen because NANOG lacks a specific TFBS in JASPAR, see Methods). This analysis identified enriched and conserved TFBS for TFs used in clustering and also identified novel TFBS (Figure 2A, S2A and Table S2). To test novel TFBS predictions for TFs not considered core pluripotency regulators, available ChIP-seq data for TFs that bind these TFBS were evaluated. Three TFs associated with TFBS enriched in CHEF regions (PRDM14, ZFX, E2F1) displayed enriched binding in CHEF, CMEF and msHEF regions compared to CLEF regions ($P<0.0001$, hypergeometric test, Figure 2B, S2B). In the case of MTF2, a known repressor (Zhang et al., 2011b), the TFBS had a negative LASSO coefficient indicating these sequences are depleted from CHEF. Consistent with this finding, ChIP-seq peaks for MTF2 are significantly depleted in CHEF regions compared to CLEF regions ($P<0.0001$, hypergeometric test, Figure 2B). These results indicate that predicted novel TFs are important for enhancer activity in ESCs.

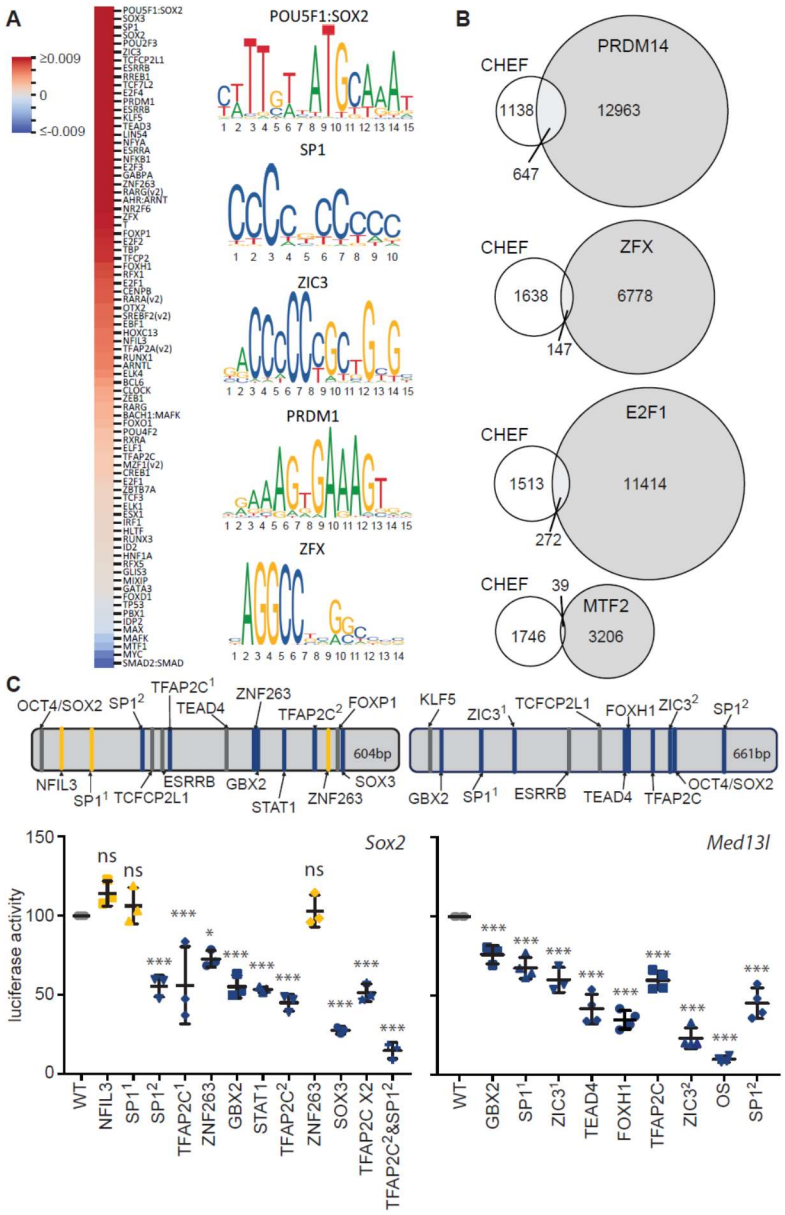

Figure 2: A large repertoire of transcription factor binding sequences are required for enhancer activity. A) Heatmap indicating diverse TFBS enriched (positive LASSO coefficients, red) or depleted (negative LASSO coefficients, blue) in CHEF regions compared to the NANOG bound CLEF regions. B) Overlap between CHEF regions and ChIP-seq peaks for TFs predicted to bind CHEF regions based on TFBS enrichment (PRDM14, E2F1, ZFX) or predicted not to bind CHEF regions based on TFBS depletion (MTF2). C) Enhancers that regulate *Sox2* or *Med13l* contain multiple conserved TFBS (top) which are required for activity as demonstrated by TFBS mutagenesis (bottom). TFBS indicated in blue were required for enhancer activity. TFBS indicated in grey were not modified, yellow indicates TFBS found not to be required for activity. Significant differences compared to the wild type (WT) sequence are indicated by * P<0.05, or *** P<0.001, ns = not significant. Error bars represent standard deviation.

To investigate the function of specific TFBS, we mutated conserved TFBS in two validated ESC enhancers, both of which are bound by six or more TFs (*Sox2* and *Med13l* enhancers, (Moorthy et al., 2017; Zhou et al., 2014), Figure S2C/D). In both enhancers, we determined that several of the novel, conserved TFBS, enriched in CHEF regions, are required for enhancer activity (Figure 2C). Although the *Sox2* enhancer contained six different conserved TFBS confirmed to be important for activity, co-mutation of only two TFBS (TFAP2C and SP1) completely abolished enhancer activity (Figure 2C). In addition to TFBS bound by the nine pluripotency TFs initially considered, additional TFBS (TFAP2C, SP1, ZNF263, GBX2, ZIC3, TEAD4, and FOXH1) were found to be important, indicating there is a large repertoire of TFBS that contribute to enhancer activity in pluripotent cells.

Additional TFBS confer gain of function to an inactive transcription factor bound region

To test if a diversity of TFBS could confer gain of function to an inactive TF bound region we evaluated a cluster of regions downstream of *Sall1*. Deletion of the entire cluster affected only *Sall1* transcription determined by RNA-seq (Moorthy et al., 2017), indicating *Sall1* is the only regulated gene for this cluster. Within the cluster (ΔEC) there are three separate TF bound regions designated as multiple TF bound loci (MTL, Figure 3A). Only two of these MTL have enhancer activity in a reporter assay or by genomic deletion (Figure 3B/C). In addition, *Sall1* transcript abundance after deletion of both MTL40 and 28 did not differ from deletion of the entire cluster indicating MTL52 has no independent enhancer activity (Figure S3). Within a core region of MTL52, 6 different TFs bind at an overlapping region, whereas the active MTL (40/28) are each bound by 9 TFs. We hypothesized MTL52 remained below a required TFBS diversity threshold, but that enhancer activity could be gained by adding a limited number of TFBS. Addition of three TFBS: ESRRB, TFCP2L1 and SMAD1 (Figure 3D, +ETS); or TFCP2L1, SMAD1 and E2F1 (Figure 3D, +TS+E2F1) to the MTL52 core region caused significantly increased enhancer activity, whereas addition of only two TFBS was not sufficient (+TS, Figure 3D). These data indicate that diversity and abundance of different TFBS are required for enhancer activity, but there is flexibility in TFBS usage.

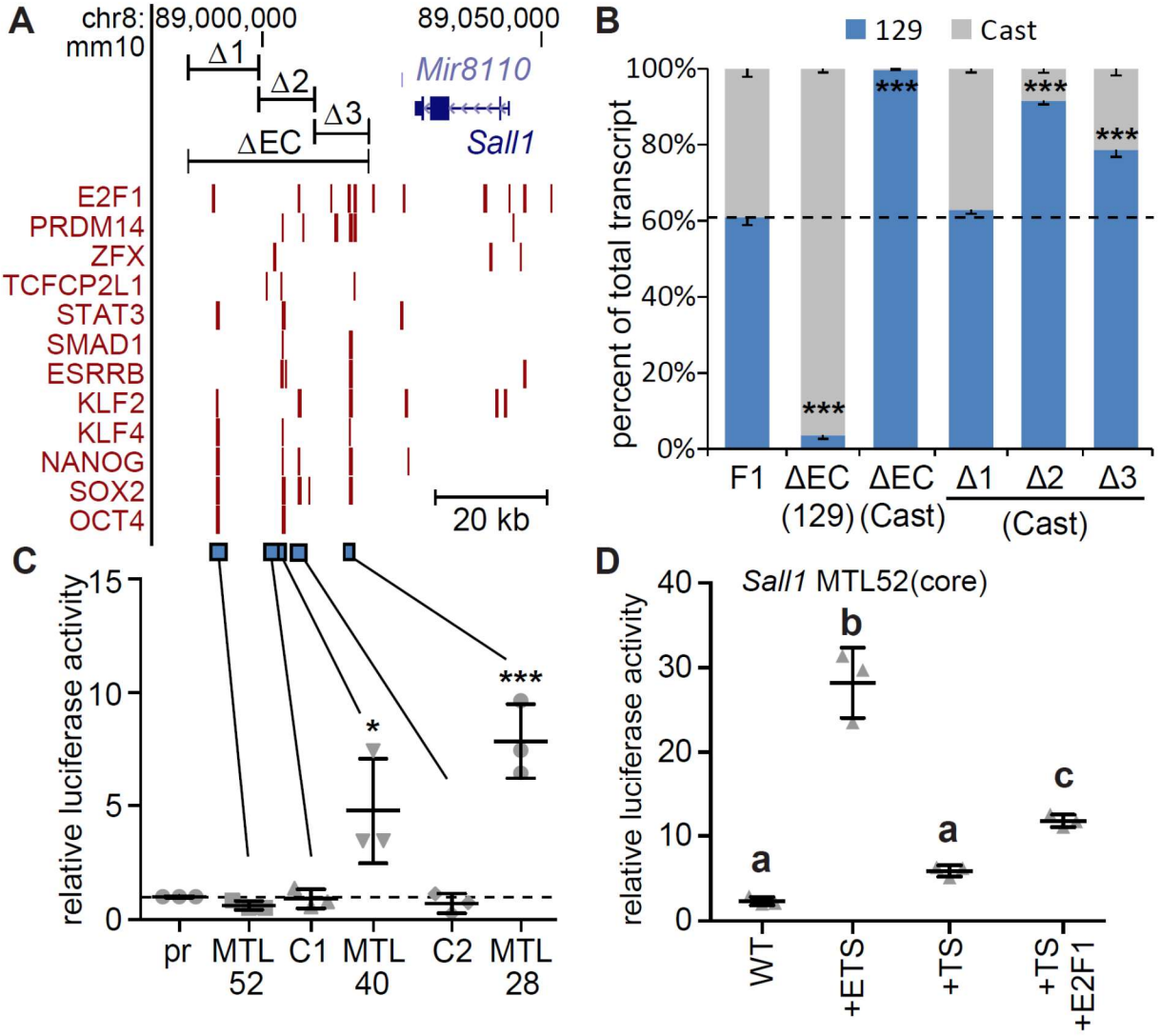

Figure 3: Addition of three different transcription factor binding sequences confers activity to an inactive region bound by six transcription factors. A) Transcription factor bound regions in the *Sall1* locus from ChIP-seq (red bars) are displayed on the mm10 assembly of the University of California at Santa Cruz (UCSC) Genome Browser. At the top CRISPR deleted regions (ΔEC, Δ1, Δ2, Δ3) are displayed. At the bottom regions tested for enhancer activity are displayed (blue bars). B) *Sall1* expression in wild type F1 clones (F1) compared to clones with the indicated deletion. Allele-specific primers detect 129 or Cast RNA in RT-qPCR. Expression for each allele is shown relative to the total. Error bars represent SEM, n≥3 biological replicates. Significant differences from the F1 values are indicated by *** P < 0.001. In C/D n≥3 biological replicates. C) Luciferase activity at control (C1, C2) regions and multiple transcription factor bound loci (MTL) 52, 40 and 28 kb downstream of *Sall1*. Error bars represent standard deviation. Significant differences from pr (promoter only) were determined by t-test and are indicated by * P <0.05, *** P<0.001. D) Luciferase activity for wild type (WT) MTL52 core TF bound region, MTL52 core with ESRRB, TCFCP2L1, and SMAD1 (+ETS) motifs mutated to the consensus TFBS. From +ETS, ESRRB (+TS) were removed. E2F1 was added to +TS (+TS+E2F1). Error bars represent standard deviation, groups determined by one-way ANOVA to be significantly different (P <0.05) are labelled with different letters.

The construction of synthetic enhancers reveals transcription factor binding site diversity is required and sufficient for robust enhancer activity

We hypothesized that if TBFS diversity from a large repertoire is sufficient for activity, we should be able to construct synthetic enhancers based on this model. Synthetic sequences containing consensus TFBS separated by 2bp spacers were constructed for evaluation in reporter assays. We selected TFBS enriched in CHEF regions and created three synthetic enhancers, each containing a different set of 14 TFBS (Table S3). All three sequences displayed robust enhancer activity, comparable to the native *Sox2* enhancer, and significantly higher than a synthetic sequence containing 14 copies of the OCT4:SOX2 co-motif ($P<0.001$, ANOVA, Figure 4A), supporting a heterotypic enhancer model in which sequences composed entirely of repeated TFBS should not act as enhancers. One of the synthetic sequences (14dTFBS_a) contains the OCT4:SOX2 co-motif; however, this motif is dispensable for enhancer activity as the other two synthetic enhancers (14dTFBS_b and 14dTFBS_c) lacked OCT4 and SOX2 motifs (Figure 4A). Previous optimization of synthetic sequences, containing KLF4, SOX2, OCT4 and ESRRB TFBS, identified two ordered combinations with the highest activity by MPRA (ksOE and sOKE)(Fiore and Cohen, 2016; King et al., 2020). Compared to our synthetic enhancers containing 14 different TFBS and to the native enhancer, these optimized 4TFBS sequences displayed significantly less activity ($P<0.01$, ANOVA, Figure 4A), suggesting 4 TFBS is below the required diversity threshold for robust activity even when an optimized regulatory grammar is used. Although there is flexibility in the specific TFBS required for activity, any 14 TFBS combination corresponding to ESC expressed TFs do not function to produce enhancer activity, as a sequence constructed from 14 different TFBS, each with a LASSO coefficient of ≤0 (14dTFBS LASSO≤0) had no activity (Figure 4A).

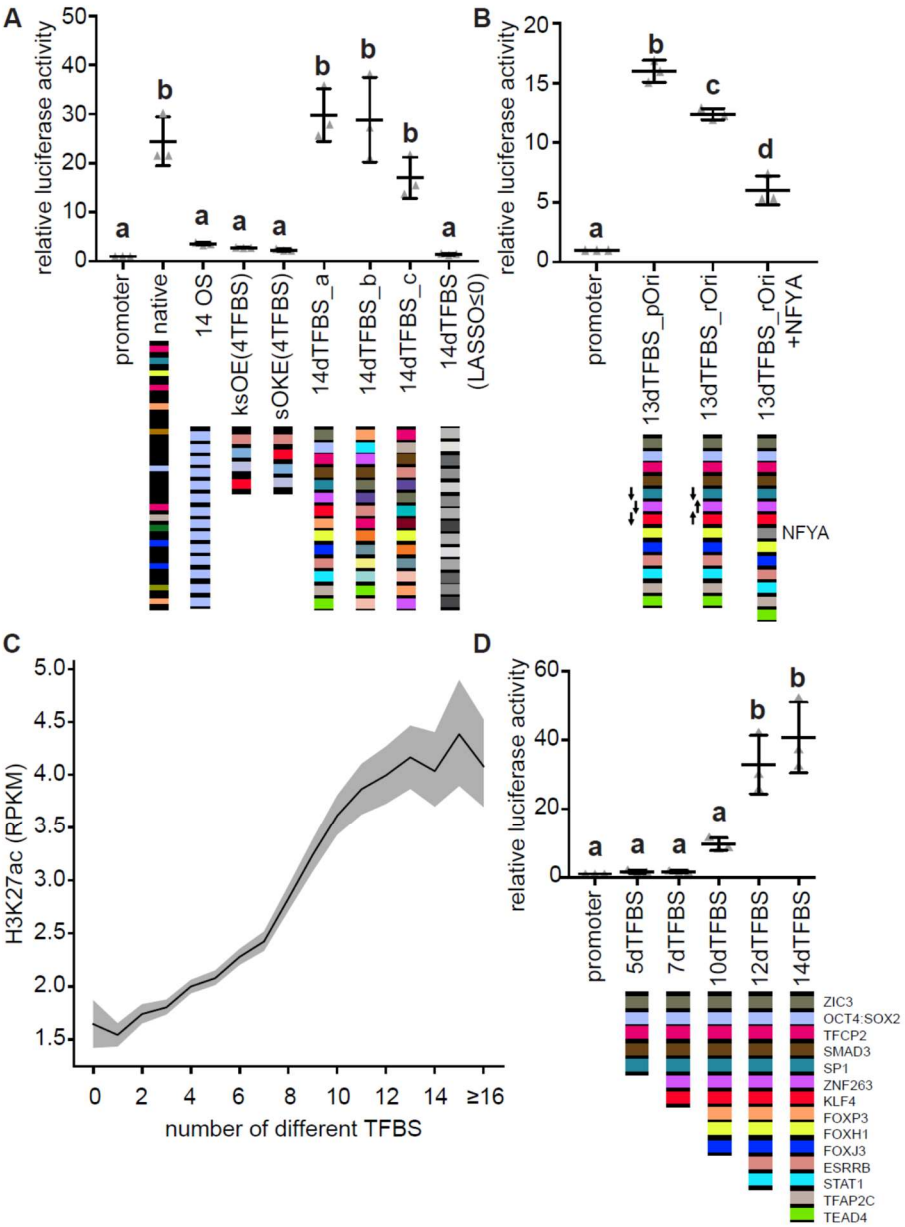

Figure 4: Transcription factor binding site diversity is required and sufficient for robust enhancer activity. In A/B/D error bars represent standard deviation, groups determined by one-way ANOVA to be significantly different (P <0.05) are labelled with different letters, n≥3 biological replicates. A) Synthetic enhancers were evaluated in reporter assays and compared to the activity of the *Sox2* enhancer (native). A sequence containing 14 OCT4:SOX2 TFSB (14 OS), optimized 4 TFBS sequences (ksOE, sOKE), or sequences containing 14 different TFBS (14dTFBS) from the LASSO enriched TFBS (a, b, c) or depleted TFBS (14dTFBS, LASSO≤0). B) Motif orientation and repressor binding affect enhancer activity. 13dTFBS_pOri contains the preferred orientation, 13dTFBS_rOri contains reversed TFBS. Addition of the repressor NFYA to 13dTFBS_rOri affects but does not abolish enhancer activity. C) A segmented threshold relationship between the number of different TFBS and H3K27ac flanking TF bound regions. D) Sequential addition of TFBS to form 14dTFBS_a revealed the importance of multiple TFBS for enhancer activity and the threshold requirement of >10 TFBS.

Although we were able to construct active synthetic enhancers by randomly ordering the selected TFBS, we also identified distance and orientation bias for a limited subset of enriched TFBS pairs within CHEF sequences that may reflect regulatory grammar (Table S4). For example, ZNF263 showed orientation bias with SP1 and KLF4 ($P<0.001$, Binomial Test). A synthetic sequence containing 13 TFBS with the preferred orientation for this pair (13dTFBS_pOri) produced significantly higher activity than the reversed orientation (13dTFBS_rOri, Figure 4B). FOXJ3 and FOXH1 are more often distant from NFYA in CHEF sequences (Table S4), suggesting pairing the NFYA TFBS with FOXJ3 and FOXH1 could disrupt enhancer activity. This is supported by the observation that NFYA can act as a repressor in combination with specific interaction partners (Peng and Jahroudi, 2002). We placed the NFYA binding sequence adjacent to FOXH1 and FOXJ3 (13dTFBS_rOri+NFYA) and observed a significant reduction in enhancer activity compared to 13dTFBS_rOri (Figure 4B). These data indicate regulatory grammar can affect enhancer activity but has a subtle effect which may fine tune gene expression.

Mutagenesis of the *Sox2* and *Med13l* enhancers, as well as addition of TFBS to the *Sall1* MTL52 suggested a threshold number of TFBS are required for enhancer activity. To test this model, we compared H3K27ac flanking TF bound regions, which is correlated with enhancer activity (Moorthy et al., 2017), to the number of different TFBS contained within each sequence, considering the TFBS enriched in CHEF regions (LASSO coefficient >0.001, Table S2). This analysis revealed sequences with only a few different CHEF-enriched TFBS have low H3K27ac whereas sequences with a greater diversity of different TFBS from this set display higher H3K27ac (Figure 4C). The relationship between these two features fits a segmented threshold model ($P = 3.266E-26$) supporting the idea of a TFBS threshold as a determinant of enhancer activity. This relationship is lost when the full set of ESC expressed or all JASPR motifs are used (Figure S4). To test the TFBS threshold experimentally, we evaluated synthetic sequences with an increasing number of different TFBS (Figure 4D). Sequences with 5, 7 and 10 different TFBS did not display significant activity whereas sequences with 12 and 14 different TFBS did. Each of these sequences contains the OCT4:SOX2 TFBS and although this TFBS is the most overrepresented in the CHEF regions, 11 additional different TFBS are required for

activity (12dTFBS, Figure 4D, Table S3). Together these data indicate that highly heterotypic sequences containing a strong consensus for more than 10 of PRDM1/14, ZFX, E2F1, TFAP2C, FOXJ3/H1/P1, SP1, ZNF263, GBX2, ZIC3, TEAD3/4, OCT4, SOX2, NANOG, ESRRB, KLF2/4/5, STAT1/2/3, or SMAD1 are likely to be strong enhancers in ESCs.

DISCUSION

Based on these data we propose a regulatory code for naïve pluripotent stem cells that requires more than 10 TFBS from the large repertoire of TFBS enriched in CHEF sequences. TFs that bind this expanded TFBS repertoire are likely to be important regulators in pluripotent cells which could drive more efficient reprogramming in combination with conventional reprogramming factors. In support of this, SP5, TFAP2C, GBX2, E2F3, ZIC3, FOXP1/FOXO1, ZFX and PRDM14 have recently been revealed as important regulators of pluripotency, self-renewal or reprogramming (Harel et al., 2012; Lim et al., 2007; Pastor et al., 2018; Seki, 2018; Tai and Ying, 2013; Tang et al., 2017, 2016; Zhang et al., 2011a).

TFBS sequence diversity above a threshold could facilitate recruitment of the large protein complexes required for transcriptional activation and elongation in mammalian cells. The mammalian mediator complex consists of 33 subunits and is required for RNA polymerase II transcription (El Khattabi et al., 2019). DNA sequences containing OCT4 TFBS act as a scaffold for phase-separated condensation of the mediator component MED1 in the nucleus (Shrinivas et al., 2019). In addition, within the set of TFs that bind the TFBS we identified as important for enhancer activity in pluripotent cells, individual TFs interact with different subcomponents of the mediator complex. SOX2 associates with MED22, NANOG with MED12, FOXJ3 with MED4 and 23, SMAD1 with MED6, 15, and 24, and ESRRB associates with several of the mediator complex proteins (Warde-Farley et al., 2010). Mediator recruitment could be facilitated by sequences that bind multiple TFs, each able to associate with different components of the complex.

Although examples exist where regulatory grammar is critical for activity as proposed by the enhanceosome model (Thanos and Maniatis, 1995), our findings indicate TFBS diversity above a threshold has a greater impact on enhancer activity. Previous studies support the observation that heterotypic sequences containing 4-6 different TFBS have increased regulatory activity compared to sequences with fewer TFBS (Fiore and Cohen, 2016; King et al., 2020; Lloret-Fernández et al., 2018). In addition, two studies assaying genomic sequences containing 4-6 different TFBS found only 28-37% of these possessed enhancer activity suggesting additional TFBS present in the active sequences confer activity (King et al., 2020; Lloret-Fernández et al., 2018). The FOXP1 TFBS, a member of our TFBS repertoire, was identified as one of the TFBS enriched in the genomic sequences displaying enhancer activity by King et al. 2020. We have now shown that more than 10 different TFBS are required for activity equivalent to a native enhancer, and that these TFBS can be drawn randomly from a large repertoire.

The observation that there is a large repertoire of TFBS that can be flexibly used to support enhancer activity without the need for optimized regulatory grammar explains the difficulty in identifying a specific regulatory code in mammalian genomes. A recent study in B-cells using STARR-seq couple with FAIRE-seq identified 43 TFBS significantly enriched in B-cell enhancers (Chaudhri et al., 2019). Comparing these B-cell TFBS with the pluripotent cell TFBS repertoire we identified, revealed only 14% overlap, suggesting a large cell-type specific TFBS repertoire confers context dependent enhancer activity. Flexible usage of TFBS from a larger tissue-specific repertoire can bypass the need for a specific individual regulator. This is supported by a recent study showing OCT4 can be excluded from the set of reprogramming TFs without limiting reprogramming efficiency (Velychko et al., 2019). Our work also reinforces the idea that master-regulator TFs are an over-simplification and instead these regulators are part of a larger and complex 'Gene Regulatory Network' where inputs from all TFs in the network are similarly important (Singh et al., 2014). Deciphering the TFBS repertoire in pluripotent stem cells supported the design of short synthetic enhancers which allow for fine-tuned control of gene expression in biotechnology and regenerative medicine contexts. Determining the repertoire of specific TFBS important for enhancer activity in different cell types will inform

a more mechanistic understanding of how specific enhancer SNPs affect gene expression and are linked to disease.

Experimental Procedures

Analysis of conserved transcription factor bound regions

Transcription factor ChIP-seq data for mouse and human was obtained from ESCODE in the CODEX database and GEO (Table S5)(Sánchez-Castillo et al., 2014; Tsankov et al., 2015). Mouse TF bound regions were identified from 16 files representing binding of nine TFs (OCT4, SOX2, NANOG, KLF4, KLF2, ESRRB, SMAD1, STAT3, and TCFCP2L1). Human TF bound regions were obtained from 9 files representing binding of seven TFs (OCT4, SOX2, NANOG, KLF5, SMAD1, STAT3 and TCF4). Overlapping TF bound regions were identified within 1kb windows. Mouse-human syntenic regions were identified using liftOver (-minMatch=0.1)(Kuhn et al., 2013). The human sequences were extended by 1kb from the mid-point to identify conserved TF binding using BEDTools(Quinlan and Hall, 2010). ChIP-seq data was retrieved for H3K27ac (GSE47949)(Wamstad et al., 2012) and EP300 (GSE24164)(Creyghton et al., 2010) in mouse ESC or H3K27ac in naïve human ESCs (GSE52824)(Gafni et al., 2013). The reads were mapped to respective genomes (mm10 and hg19) using Bowtie(Langmead et al., 2009). RPKM values for H3K27ac ChIP/input were calculated for 2kb regions surrounding TF bound region midpoints. Venn diagrams were created using 'eulerr' in R(Micallef and Rodgers, 2014).

To focus on conserved distal regulatory regions the 23,830 TF bound regions in mouse that aligned to the human genome after excluding promoters (transcription start site, TSS -2 kb) were clustered into 9 clusters. The H3K27ac ChIP-Seq signal was assumed to follow a Gaussian distribution, whereas binding of each TFs were assumed to follow Bernoulli distributions. The sums of mouse & human TFs (TF sum) were assumed to follow Poisson distributions. To optimize parameters of the mixture model, we used the expectation maximization algorithm, which requires initial parameter values. We used Behrouz Babaki's implementation of constrained k-means (https://github.com/Behrouz-

Babaki/COP-Kmeans)(Wagstaff et al., 2001) to generate initial clusters. Using 'pomegranate' package, initial parameter values of distributions (mean & standard deviation) were calculated from clusters and 'IndependentComponentsDistribution' was used to create a multivariate distribution. Gaussian Mixture models (GMMs) was used to fit and predict the clusters of enhancers using unsupervised learning. For the clusters' visualization, heatmap was generated using the 'seaborn' package in which each feature is scaled from 0 to 1. The cluster output with the lowest Bayesian information criterion (BIC) was chosen as the final cluster.

TFBS conservation and enrichment analysis

TFBS analysis was carried out for sequences within each cluster and random intergenic regions selected from regions not bound to any TF in mouse or human ESCs. Any region overlapping an exon or 2kb upstream of a TSS was removed as these sequences are often highly conserved. Using 700bp of sequence centered on the midpoint of the TF bound region (or sequence midpoint for non-TF bound regions) in the mouse genome, the corresponding syntenic regions in the human, rhesus macaque, mouse, rat, cow and pig genomes were identified using liftOver. After liftOver the sequence was expanded to 2kb prior to multi-sequence alignment (MSA). MSA was performed using Mafft (Katoh and Standley, 2013) E-INS-I (Iterative refinement method) with the 'adjustdirectionaccurately' feature. MSA was trimmed on both 5' and 3' ends to best match the 700bp mouse reference sequence with respective aligned sequences from the other five species. The mouse sequence was scanned for TFBS with a relative profile threshold of 90% for all 519 non-redundant JASPAR profiles by using 'searchSeq' in 'TFBSTools'(Tan and Lenhard, 2016) and the 'JASPAR2016' (Mathelier et al., 2016) package in R. For purifying selection pressure analysis in CHEF cluster, putative sites with score >11 for each JASPAR PWM were evaluated. Human-mouse percent identity for each TFBS was calculated using TFBSTools identified motifs in the mouse sequence. The corresponding sequences for human were then identified in the MSA. TFBS conservation was calculated as average percentage identity between mouse and human of all motifs for each individual PWM. Scrambled PWM for all 519 JASPAR profiles were created using 'permuteMatrix' in 'TFBSTools' (Tan and Lenhard, 2016) and then those

scrambled PWM were scanned in the mouse sequence for CHEF regions and mouse-human percentage identity was calculated as described above to identify scrambled TFBS conservation.

The 700 bp trimmed six species MSA for each of the regions in the 9 clusters and random regions was used as input for MotEvo with mouse as the reference sequence. Input parameters for MotEvo included nucleotide percentage and averaged phylogenetic tree for all six species which were calculated using the MSA of CHEF regions. Phylogenetic trees were generated using PhyML (Guindon et al., 2010) for those MSA with liftOver sequences in all six species. MotEvo analysis was performed using refspecies Mouse; Mode: TFBS; EMprior: 0; markovorderBG: 0; minposterior: 0.2. Motevo output resulted in posterior probabilities for each of the 349 redundant PWM belonging to expressed TFs in ESCs (log RPKM≥0.25, RNA-Seq from GSE79313 (Moorthy et al., 2017)), which were used as features in machine learning to distinguish CHEF sequences from the NANOG cluster. To rank and select important features, LASSO (Least Absolute Shrinkage and Selection Operator) was used with the Scikit-learn (Pedregosa et al., 2011) Python module. LassoLarsCV with 10-fold cross validation was used to identify the parameter (-log[alpha]) which generated the highest classification accuracy which was then used for feature selection.

To determine the number of conserved different TFBS present in cluster regions the number of different MotEvo identified motifs, from the set of 349 TFBS, were counted in each sequence. To determine if conserved TFBS are present in addition to any corresponding to the 9 TFs used for cluster analysis, the number of different MotEvo identified motifs, from a reduced set of 309 TFBS, were counted in each sequence.

A selected set of 62 TFBS with LASSO logistic regression coefficient >0.001 and significantly different TFBS from each other (Pearson correlation coefficient ≤0.5) were chosen to identify the number of different TFBS present within a 700bp window for all TF bound regions. Motifs with score >11 as described above were identified using TFBSTools. The relationship between the number of different TFBS and H3K27ac in the

2kb flanking regions was plotted using lineplot in the 'seaborn' package in python3.6. Using R, log likelihood was calculated for a linear regression model and a segmented threshold model from 'segmented' package(Muggeo, 2017), P value was calculated using the likelihood ratio test (LRT) with a $\chi 2$ distribution. For comparison, the set of all 519 JASPAR motifs, or the 349 JASPR motifs corresponding to ESC expressed TFs were used to identify the number of TFBS in each sequence and the relationship to flanking H3K27ac (Figure S4).

Site-directed mutagenesis

For the analysis of conserved TFBS in the *Sox2* and *Med13l* enhancers, the two nucleotides in the motif with the highest score in the consensus were mutated to non-consensus nucleotides. The effect of the mutation was tested using TFBSTools to confirm that it disrupted the reference TFBS without creating another TFBS for an ESC expressed TF. Mutations in enhancer sequences in pGL4.23 vector were introduced using the QuickChange Lightening kit (Agilent) with the primers described in Table S6. For the gain of function analysis in the *Sall1* MTL52 sequence we focused on the smaller core region bound by six TFs (MTL52core). We identified motifs with the closest match to the desired TFBS, as these all had a low consensus match score, the identified motifs were mutated in the MTL52core sequence using Gibson Assembly to produce the consensus sequence for ESRRB, TFCP2L1, and SMAD1 (+ETS). In the +ETS sequence, ESRRB motif was mutated to non-consensus nucleotides preventing binding of any other TF at this region to create +TS. Another gain of function construct +TS+E2F1 was created by adding a strong consensus motif for E2F1 to the +TS construct using the QuickChange Lightening kit (Agilent). For the gain of function TFBS analysis, a maximum of six mutations were introduced, using the primers described in Table S6, to convert a non-consensus motif into a strong consensus motif for the desired TFBS.

Cell culture and CRISPR deletion

F1 mouse ES cells (*M. musculus*^{129} × *M. castaneus*, obtained from Barbara Panning) were cultured on 0.1% gelatin-coated plates in ESC media (DMEM containing 15% FBS, 0.1 mM MEM nonessential amino-acids, 1 mM sodium pyruvate, 2 mM GlutaMAX, 0.1

mM 2-mercaptoethanol, 1000 U/mL LIF, 3 μM CHIR99021 [GSK3β inhibitor; Biovision], and 1 μM PD0325901 [MEK inhibitor; Sigma Aldrich]), to maintain the naïve state. Cas9 targeting guides flanking *Sall1* proximal TF bound regions were selected (Table S7). Only gRNAs predicted to have no off-target binding in the mouse genome were chosen. Guide RNA plasmids were assembled in the gRNA empty vector (Addgene, ID#41824) using the protocol described by Mali et. al. (2013)(Mali et al., 2013) and confirmed by sequencing. Following the protocol described in Moorthy et. al. (2016)(Moorthy and Mitchell, 2016), 5 μg each of the indicated gRNAs targeting the 5' and 3' ends of the TF bound region were transfected in ESCs with pCas9_GFP (Addgene, ID#44719)(Ding et al., 2013) using the Neon Transfection System (Life Technologies). FACS sorting 48-hous post-transfection isolated GFP-positive cells, which were collected and seeded on 10-cm gelatinized culture plates. Genotyping of enhancer deletions was done by qPCR with allele-specific primers. All deletions were confirmed by sequence analysis using primers 5′ of and 3′ from the gRNA target sites; SNPs within the amplified product confirmed the genotype of the deleted allele. Gene expression was monitored by RT-qPCR using allele-specific primers (Sall1_129, Sall1_Cast) that distinguish 129 from *castaneus* alleles (Table S6). The standard curve method was used to calculate expression levels, with mouse F1 genomic DNA used to generate the standard curves.

Synthetic sequences, enhancers and luciferase assay

Synthetic enhancer sequences as described in Table S3 were generated as GenPart DNA Fragments (GenScript). These sequences contained 2bp 'CC' spacers between each TFBS. For the creation of 14dTFBS LASSO≤0, only TFBS that were significantly different (Pearson correlation coefficient ≤0.5) from LASSO+ TFBS were used. Using the conserved motifs for selected TFBS identified from the MotEvo analysis, the distance and orientation between each pair of TFBS was averaged over all CHEF sequences to identify the average co-occurrence distance and preferred orientation between each TFBS pair. If more than one motif per TFBS were present, the orientation present in ≥66% motifs was chosen as reference otherwise it was excluded. Significance of orientation bias was calculated by Binomial Test, with the null hypothesis being no bias, 50% occurrence probability for either orientation.

To evaluate enhancer activity, synthetic sequences or native TF bound regions were cloned downstream of the firefly luciferase gene at the *NotI* site in the pGL4.23 vector containing an *Oct4* minimal promoter as described in Moorthy et. al. (2017)(Moorthy et al., 2017). Mouse F1 ESCs were seeded on gelatin coated 96-well plates at a density of 10,000 cells per well. After 24 hours the cells were co-transfected using jetPRIME (VWR International) with pGL4.23 vectors and a *Renilla* luciferase encoding plasmid (pGL4.75) at a 50:1 molar ratio. Renilla plasmid is transfected as control for transfection efficiency in each well. ESC media was replaced with fresh ESC media after 24 hours. Luciferase activity was assayed 48 hours post transfection using a dual luciferase reporter assay (Promega) and the firefly/Renilla ratio was measured on the Fluoroskan Ascent FL plate reader. All experiments were done in ≥3 biological replicates with each experiment having ≥3 technical transfection replicates.

Author Contributions

G.S. and J.A.M. conceived the project, designed the experiments, and analyzed all experimental data. A.M.M. contributed to the design and analysis for computational approaches. G.S. performed the experiments in Figures 1, 2, 4, S1, S2 and S4. S.M. performed the experiments in Figures 3D and 4A. S.D.M. performed the experiments in Figures 3B and S3B. R.Z. performed the experiments in Figure 2C. T.M. performed the experiments in Figure 1B. V.M.S. performed the experiments in Figure 3C. R.T. performed the experiments in Figure 3D. G.S. and J.A.M. wrote the manuscript, which was approved by all coauthors.

ACKNOWLEDGMENTS

We would like to thank all the members of the Mitchell and Moses labs for helpful discussions. This work was supported by Natural Science and Engineering Research Council of Canada, the Canada Foundation for Innovation, and the Ontario Ministry of Research and Innovation (operating and infrastructure grants held by J.A.M.). Studentship funding to support this work was provided by Connaught International Scholarships and Ontario Graduate Scholarship (G.S.), and Natural Sciences and Engineering Research Council of Canada Scholarships (V.M.S.). Salary support for S. D. M. was provided by Canadian Institutes of Health Research Project Grant (FRN 153186).

References

Arnold, P., Erb, I., Pachkov, M., Molina, N., and van Nimwegen, E. (2012). MotEvo: integrated Bayesian probabilistic methods for inferring regulatory sites and motifs on multiple alignments of DNA sequences. Bioinformatics *28*, 487–494.

Ballester, B., Medina-Rivera, A., Schmidt, D., Gonzàlez-Porta, M., Carlucci, M., Chen, X., Chessman, K., Faure, A.J., Funnell, A.P.P.W., Goncalves, A., et al. (2014). Multi-species, multi-transcription factor binding highlights conserved control of tissue-specific biological pathways. Elife *3*, 1–29.

Barakat, T.S., Halbritter, F., Zhang, M., Rendeiro, A.F., Perenthaler, E., Bock, C., and

Chambers, I. (2018). Functional Dissection of the Enhancer Repertoire in Human Embryonic Stem Cells. Cell Stem Cell *23*, 276-288.e8.

Bernstein, B.E., Birney, E., Dunham, I., Green, E.D., Gunter, C., and Snyder, M. (2012). An integrated encyclopedia of DNA elements in the human genome. Nature *489*, 57–74.

Chaudhri, V.K., Dienger-Stambaugh, K., Wu, Z., Shrestha, M., and Singh, H. (2019). Charting the cis-regulome of activated B cells by coupling structural and functional genomics. Nat. Immunol.

Chen, C.Y., Morris, Q., and Mitchell, J.A. (2012). Enhancer identification in mouse embryonic stem cells using integrative modeling of chromatin and genomic features. BMC Genomics *13*, 152.

Chen, L., Fish, A.E., and Capra, J.A. (2018). Prediction of gene regulatory enhancers across species reveals evolutionarily conserved sequence properties. PLOS Comput. Biol. *14*, e1006484.

Chen, X., Xu, H., Yuan, P., Fang, F., Huss, M., Vega, V.B., Wong, E., Orlov, Y.L., Zhang, W., Jiang, J., et al. (2008). Integration of External Signaling Pathways with the Core Transcriptional Network in Embryonic Stem Cells. Cell *133*, 1106–1117.

Corces, M.R., Granja, J.M., Shams, S., Louie, B.H., Seoane, J.A., Zhou, W., Silva, T.C., Groeneveld, C., Wong, C.K., Cho, S.W., et al. (2018). The chromatin accessibility landscape of primary human cancers. Science *362*, eaav1898.

Creyghton, M.P., Cheng, A.W., Welstead, G.G., Kooistra, T., Carey, B.W., Steine, E.J., Hanna, J., Lodato, M.A., Frampton, G.M., Sharp, P.A., et al. (2010). Histone H3K27ac separates active from poised enhancers and predicts developmental state. Proc. Natl. Acad. Sci. U. S. A. *107*, 21931–21936.

Ding, Q., Regan, S.N., Xia, Y., Oostrom, L.A., Cowan, C.A., and Musunuru, K. (2013). Enhanced Efficiency of Human Pluripotent Stem Cell Genome Editing through Replacing TALENs with CRISPRs. Cell Stem Cell *12*, 393–394.

Ernst, J., and Kellis, M. (2012). ChromHMM: Automating chromatin-state discovery and characterization. Nat. Methods *9*, 215–216.

Farley, E.K., Olson, K.M., Zhang, W., Rokhsar, D.S., and Levine, M.S. (2016). Syntax

compensates for poor binding sites to encode tissue specificity of developmental enhancers. Proc. Natl. Acad. Sci. U. S. A. *113*, 6508–6513.

Farnham, P.J. (2012). Thematic Minireview Series on Results from the ENCODE Project: Integrative Global Analyses of Regulatory Regions in the Human Genome. J Biol Chem. *287*, 30885–30887.

Ferri, A.L.M., Cavallaro, M., Braida, D., Di Cristofano, A., Canta, A., Vezzani, A., Ottolenghi, S., Pandolfi, P.P., Sala, M., DeBiasi, S., et al. (2004). Sox2 deficiency causes neurodegeneration and impaired neurogenesis in the adult mouse brain. Development *131*, 3805–3819.

Fiore, C., and Cohen, B.A. (2016). Interactions between pluripotency factors specify cis-regulation in embryonic stem cells. Genome Res. *26*, 778–786.

Gafni, O., Weinberger, L., Mansour, A.A., Manor, Y.S., Chomsky, E., Ben-Yosef, D., Kalma, Y., Viukov, S., Maza, I., Zviran, A., et al. (2013). Derivation of novel human ground state naive pluripotent stem cells. Nature *504*, 282–286.

Guindon, S., Dufayard, J.-F., Lefort, V., Anisimova, M., Hordijk, W., and Gascuel, O. (2010). New algorithms and methods to estimate maximum-likelihood phylogenies: assessing the performance of PhyML 3.0. Syst. Biol. *59*, 307–321.

Harel, S., Tu, E.Y., Weisberg, S., Esquilin, M., Chambers, S.M., Liu, B., Carson, C.T., Studer, L., Reizis, B., and Tomishima, M.J. (2012). ZFX Controls the Self-Renewal of Human Embryonic Stem Cells. PLoS One *7*, e42302.

Katoh, K., and Standley, D.M. (2013). MAFFT multiple sequence alignment software version 7: improvements in performance and usability. Mol. Biol. Evol. *30*, 772–780.

El Khattabi, L., Zhao, H., Kalchschmidt, J., Young, N., Jung, S., Van Blerkom, P., Kieffer-Kwon, P., Kieffer-Kwon, K.-R., Park, S., Wang, X., et al. (2019). A Pliable Mediator Acts as a Functional Rather Than an Architectural Bridge between Promoters and Enhancers. Cell *178*, 1145-1158.e20.

Kheradpour, P., Ernst, J., Melnikov, A., Rogov, P., Wang, L., Zhang, X., Alston, J., Mikkelsen, T.S., and Kellis, M. (2013). Systematic dissection of regulatory motifs in 2000 predicted human enhancers using a massively parallel reporter assay. Genome

Res. *23*, 800–811.

King, D.M., Hong, C.K.Y., Shepherdson, J.L., Granas, D.M., Maricque, B.B., and Cohen, B. (2020). Synthetic and genomic regulatory elements reveal aspects of cis-regulatory grammar in Mouse Embryonic Stem Cells. Elife *9*.

Kuhn, R.M., Haussler, D., and Kent, W.J. (2013). The UCSC genome browser and associated tools. Brief. Bioinform. *14*, 144–161.

Kvon, E.Z., Kamneva, O.K., Melo, U.S., Barozzi, I., Osterwalder, M., Mannion, B.J., Tissières, V., Pickle, C.S., Plajzer-Frick, I., Lee, E.A., et al. (2016). Progressive Loss of Function in a Limb Enhancer during Snake Evolution. Cell *167*, 633-642.e11.

Kwasnieski, J.C., Fiore, C., Chaudhari, H.G., and Cohen, B.A. (2014). High-throughput functional testing of ENCODE segmentation predictions. Genome Res. *24*, 1595–1602.

Langmead, B., Trapnell, C., Pop, M., and Salzberg, S.L. (2009). Ultrafast and memory-efficient alignment of short DNA sequences to the human genome. Genome Biol. *10*, R25.

Libbrecht, M.W., Rodriguez, O.L., Weng, Z., Bilmes, J.A., Hoffman, M.M., and Noble, W.S. (2019). A unified encyclopedia of human functional DNA elements through fully automated annotation of 164 human cell types. Genome Biol. *20*, 180.

Lim, L.S., Loh, Y.-H., Zhang, W., Li, Y., Chen, X., Wang, Y., Bakre, M., Ng, H.-H., and Stanton, L.W. (2007). Zic3 Is Required for Maintenance of Pluripotency in Embryonic Stem Cells. Mol. Biol. Cell *18*, 1348–1358.

Lloret-Fernández, C., Maicas, M., Mora-Martínez, C., Artacho, A., Jimeno-Martín, Á., Chirivella, L., Weinberg, P., and Flames, N. (2018). A transcription factor collective defines the HSN serotonergic neuron regulatory landscape. Elife *7*.

Lusk, R.W., and Eisen, M.B. (2010). Evolutionary Mirages: Selection on Binding Site Composition Creates the Illusion of Conserved Grammars in Drosophila Enhancers. PLoS Genet. *6*, e1000829.

Mali, P., Yang, L., Esvelt, K.M., Aach, J., Guell, M., DiCarlo, J.E., Norville, J.E., and Church, G.M. (2013). RNA-guided human genome engineering via Cas9. Science *339*, 823–826.

Mathelier, A., Fornes, O., Arenillas, D.J., Chen, C., Denay, G., Lee, J., Shi, W., Shyr, C., Tan, G., Worsley-Hunt, R., et al. (2016). JASPAR 2016: a major expansion and update of the open-access database of transcription factor binding profiles. Nucleic Acids Res. *44*, D110–D115.

Maurano, M.T., Humbert, R., Rynes, E., Thurman, R.E., Haugen, E., Wang, H., Reynolds, A.P., Sandstrom, R., Qu, H., Brody, J., et al. (2012). Systematic Localization of Common Disease-Associated Variation in Regulatory DNA. Science (80-.). *337*, 1190–1195.

McLean, C.Y., Reno, P.L., Pollen, A.A., Bassan, A.I., Capellini, T.D., Guenther, C., Indjeian, V.B., Lim, X., Menke, D.B., Schaar, B.T., et al. (2011). Human-specific loss of regulatory DNA and the evolution of human-specific traits. Nature *471*, 216–219.

Micallef, L., and Rodgers, P. (2014). eulerAPE: Drawing Area-Proportional 3-Venn Diagrams Using Ellipses. PLoS One *9*, e101717.

Moorthy, S.D., and Mitchell, J.A. (2016). Generating CRISPR/Cas9 Mediated Monoallelic Deletions to Study Enhancer Function in Mouse Embryonic Stem Cells. J. Vis. Exp. e53552.

Moorthy, S.D., Davidson, S., Shchuka, V.M., Singh, G., Malek-Gilani, N., Langroudi, L., Martchenko, A., So, V., Macpherson, N.N., and Mitchell, J.A. (2017). Enhancers and super-enhancers have an equivalent regulatory role in embryonic stem cells through regulation of single or multiple genes. Genome Res. *27*, 246–258.

Muggeo, V.M.R. (2017). Interval estimation for the breakpoint in segmented regression: a smoothed score-based approach. Aust. New Zeal. J. Stat. *59*, 311–322.

Murtha, M., Tokcaer-Keskin, Z., Tang, Z., Strino, F., Chen, X., Wang, Y., Xi, X., Basilico, C., Brown, S., Bonneau, R., et al. (2014). FIREWACh: High-throughput functional detection of transcriptional regulatory modules in mammalian cells. Nat. Methods *11*, 559–565.

Pastor, W.A., Liu, W., Chen, D., Ho, J., Kim, R., Hunt, T.J., Lukianchikov, A., Liu, X., Polo, J.M., Jacobsen, S.E., et al. (2018). TFAP2C regulates transcription in human naive pluripotency by opening enhancers. Nat. Cell Biol. *20*, 553–564.

Pedregosa, F., Varoquaux, G., Gramfort, A., Michel, V., Thirion, B., Grisel, O., Blondel, M., Prettenhofer, P., Weiss, R., Dubourg, V., et al. (2011). Scikit-learn: Machine Learning in Python. J. Mach. Learn. Res. *12*, 2825–2830.

Peng, Y., and Jahroudi, N. (2002). The NFY transcription factor functions as a repressor and activator of the von Willebrand factor promoter. Blood *99*, 2408–2417.

Prescott, S.L., Srinivasan, R., Marchetto, M.C., Grishina, I., Narvaiza, I., Selleri, L., Gage, F.H., Swigut, T., and Wysocka, J. (2015). Enhancer Divergence and cis-Regulatory Evolution in the Human and Chimp Neural Crest. Cell *163*, 68–83.

Quinlan, A.R., and Hall, I.M. (2010). BEDTools: A flexible suite of utilities for comparing genomic features. Bioinformatics *26*, 841–842.

Rada-Iglesias, A., Bajpai, R., Swigut, T., Brugmann, S.A., Flynn, R.A., and Wysocka, J. (2011). A unique chromatin signature uncovers early developmental enhancers in humans. Nature *470*, 279–285.

Sánchez-Castillo, M., Ruau, D., Wilkinson, A.C.., Ng, F.S.L.., Hannah, R., Diamanti, E., Lombard, P., Wilson, N.K.., and Gottgens, B. (2014). CODEX: a next-generation sequencing experiment database for the haematopoietic and embryonic stem cell communities. Nucleic Acids Res.

Schnetz, M.P., Handoko, L., Akhtar-Zaidi, B., Bartels, C.F., Pereira, C.F., Fisher, A.G., Adams, D.J., Flicek, P., Crawford, G.E., LaFramboise, T., et al. (2010). CHD7 Targets Active Gene Enhancer Elements to Modulate ES Cell-Specific Gene Expression. PLoS Genet. *6*, e1001023.

Seki, Y. (2018). PRDM14 is a unique epigenetic regulator stabilizing transcriptional networks for pluripotency. Front. Cell Dev. Biol. *6*.

Shrinivas, K., Sabari, B.R., Coffey, E.L., Klein, I.A., Boija, A., Zamudio, A. V., Schuijers, J., Hannett, N.M., Sharp, P.A., Young, R.A., et al. (2019). Enhancer Features that Drive Formation of Transcriptional Condensates. Mol. Cell *75*, 549-561.e7.

Singh, H., Khan, A.A., and Dinner, A.R. (2014). Gene regulatory networks in the immune system. Trends Immunol. *35*, 211–218.

Smith, R.P., Taher, L., Patwardhan, R.P., Kim, M.J., Inoue, F., Shendure, J.,

Ovcharenko, I., and Ahituv, N. (2013). Massively parallel decoding of mammalian regulatory sequences supports a flexible organizational model. Nat. Genet. *45*, 1021–1028.

Tai, C.-I., and Ying, Q.-L. (2013). Gbx2, a LIF/Stat3 target, promotes reprogramming to and retention of the pluripotent ground state. J. Cell Sci. *126*, 1093–1098.

Tan, G., and Lenhard, B. (2016). TFBSTools: an R/bioconductor package for transcription factor binding site analysis. Bioinformatics *32*, 1555–1556.

Tang, L., Wang, M., Liu, D., Gong, M., Ying, Q.L., and Ye, S. (2017). Sp5 induces the expression of Nanog to maintain mouse embryonic stem cell self-renewal. PLoS One *12*.

Tang, X., Liu, H., Srivastava, A., Pécot, T., Chen, Z., Wang, Q., Huang, K., Sáenz-Robles, M.T., Cantalupo, P., Pipas, J., et al. (2016). Transcriptome regulation and chromatin occupancy by E2F3 and MYC in mice. Sci. Data *3*, 160008.

Thanos, D., and Maniatis, T. (1995). Virus induction of human IFNβ gene expression requires the assembly of an enhanceosome. Cell *83*, 1091–1100.

Tibshirani, R. (1996). Regression Shrinkage and Selection via the Lasso. J. R. Stat. Soc. Ser. B *58*, 267–288.

Tsankov, A.M., Gu, H., Akopian, V., Ziller, M.J., Donaghey, J., Amit, I., Gnirke, A., and Meissner, A. (2015). Transcription factor binding dynamics during human ES cell differentiation. Nature *518*, 344–349.

Vanhille, L., Griffon, A., Maqbool, M.A., Zacarias-Cabeza, J., Dao, L.T.M., Fernandez, N., Ballester, B., Andrau, J.C., and Spicuglia, S. (2015). High-throughput and quantitative assessment of enhancer activity in mammals by CapStarr-seq. Nat. Commun. *6*, 6905.

Velychko, S., Adachi, K., Kim, K.P., Hou, Y., MacCarthy, C.M., Wu, G., and Schöler, H.R. (2019). Excluding Oct4 from Yamanaka Cocktail Unleashes the Developmental Potential of iPSCs. Cell Stem Cell *25*, 737-753.e4.

Villar, D., Berthelot, C., Aldridge, S., Rayner, T.F., Lukk, M., Pignatelli, M., Park, T.J., Deaville, R., Erichsen, J.T., Jasinska, A.J., et al. (2015). Enhancer Evolution across 20

Mammalian Species. Cell *160*, 554–566.

Visel, A., Prabhakar, S., Akiyama, J.A., Shoukry, M., Lewis, K.D., Holt, A., Plajzer-Frick, I., Afzal, V., Rubin, E.M., and Pennacchio, L.A. (2008). Ultraconservation identifies a small subset of extremely constrained developmental enhancers. Nat. Genet. *40*, 158–160.

Visel, A., Rubin, E.M., and Pennacchio, L.A. (2009a). Genomic views of distant-acting enhancers. Nature *461*, 199–205.

Visel, A., Blow, M.J., Li, Z., Zhang, T., Akiyama, J.A., Holt, A., Plajzer-Frick, I., Shoukry, M., Wright, C., Chen, F., et al. (2009b). ChIP-seq accurately predicts tissue-specific activity of enhancers. Nature *457*, 854–858.

Visel, A., Taher, L., Girgis, H., May, D., Golonzhka, O., Hoch, R.V., McKinsey, G.L., Pattabiraman, K., Silberberg, S.N., Blow, M.J., et al. (2013). A High-Resolution Enhancer Atlas of the Developing Telencephalon. Cell *152*, 895–908.

Wagstaff, K., Cardie, C., Rogers, S., and Schroedl, S. (2001). Constrained K-means Clustering with Background Knowledge.

Wamstad, J.A., Alexander, J.M., Truty, R.M., Shrikumar, A., Li, F., Eilertson, K.E., Ding, H., Wylie, J.N., Pico, A.R., Capra, J.A., et al. (2012). Dynamic and coordinated epigenetic regulation of developmental transitions in the cardiac lineage. Cell *151*, 206–220.

Warde-Farley, D., Donaldson, S.L., Comes, O., Zuberi, K., Badrawi, R., Chao, P., Franz, M., Grouios, C., Kazi, F., Lopes, C.T., et al. (2010). The GeneMANIA prediction server: biological network integration for gene prioritization and predicting gene function. Nucleic Acids Res. *38*, W214–W220.

Zhang, X., Yalcin, S., Lee, D.-F., Yeh, T.-Y.J., Lee, S.-M., Su, J., Mungamuri, S.K., Rimmelé, P., Kennedy, M., Sellers, R., et al. (2011a). FOXO1 is an essential regulator of pluripotency in human embryonic stem cells. Nat. Cell Biol. *13*, 1092–1099.

Zhang, Z., Jones, A., Sun, C.-W., Li, C., Chang, C.-W., Joo, H.-Y., Dai, Q., Mysliwiec, M.R., Wu, L.-C., Guo, Y., et al. (2011b). PRC2 Complexes with JARID2, MTF2, and esPRC2p48 in ES Cells to Modulate ES Cell Pluripotency and Somatic Cell

Reprograming. Stem Cells *29*, 229–240.

Zhou, H.Y.., Katsman, Y., Dhaliwal, N.K.., Davidson, S., Macpherson, N.N.., Sakthidevi, M., Collura, F., and Mitchell, J.A. (2014). A Sox2 distal enhancer cluster regulates embryonic stem cell differentiation potential. Genes Dev. *28*, 2699–2711.

Zinzen, R.P., Girardot, C., Gagneur, J., Braun, M., and Furlong, E.E.M. (2009). Combinatorial binding predicts spatio-temporal cis-regulatory activity. Nature *462*, 65–70.